Chemical Kinetics of the Azide Radical: Rate Constants for Reactions with Cl, NO, NO_2, O_2, CO, CO_2, Cl_2, and C_3H_6

Kevin B. Hewett and D. W. Setser*

Department of Chemistry, Kansas State University, Manhattan, Kansas 66506

Received: April 3, 1998; In Final Form: May 27, 1998

The reactions of the azide radical ($\tilde{X}\ ^2\Pi_g$), produced by the reaction of F atoms with HN_3, with F, Cl, NO, NO_2, O_2, CO, CO_2, Cl_2, and propylene have been examined in a room-temperature flow reactor. The relative concentration of N_3 was monitored under pseudo-first-order conditions using laser-induced fluorescence. A microwave discharge applied to a dilute flow of CF_4 in argon served as the F atom source for the F + HN_3 reaction. Using reactant concentrations of (0.5−4.0) × 10^{12} and (1.0−4.0) × 10^{12} molecules cm^{-3} for CF_4 and HN_3, respectively, the rate constant for the N_3 + F reaction was found to be (4.1 ± 0.3) × 10^{-11} cm^3 $molecule^{-1}$ s^{-1}, which compares favorably with the accepted value of (5 ± 2) × 10^{-11} cm^3 $molecule^{-1}$ s^{-1}. The reaction with Cl atoms was examined using reactant concentrations of (5.5−9.4) × 10^{11}, (2.0−4.0) × 10^{12}, and (1.0−22.0) × 10^{12} molecules cm^{-3} for CF_4, HN_3, and Cl_2, respectively, and the rate constant is $(2.1^{+1.0}_{-0.6})$ × 10^{-11} cm^3 $molecule^{-1}$ s^{-1}. The rate constants for the reactions of N_3 with NO, NO_2, and CO were determined to be (2.9 ± 0.3) × 10^{-12}, (1.9 ± 0.2) × 10^{-12}, and (1.8 ± 0.2) × 10^{-12} cm^3 $molecule^{-1}$ s^{-1}, respectively. The reactions between azide radicals and Cl_2, CO_2, O_2, and propylene all occur with rate constants less than 5 × 10^{-13} cm^3 $molecule^{-1}$ s^{-1}, indicating that N_3 is not an especially reactive radical. The bimolecular self-destruction rate for azide radical was also examined. An upper bound on the rate constant was determined to be ≤1−2 × 10^{-12} cm^3 $molecule^{-1}$ s^{-1}. The possible products and the reaction mechanisms of these reactions are discussed.

A. Introduction

The azide radical, $N_3(\tilde{X}\ ^2\Pi_g)$, has been the subject of a variety of theoretical[1−4] and experimental[4−26] studies with regard to electronic structure and reactions with halogen atoms. The enthalpy of formation for the azide radical has been determined to be $\Delta_f H^\circ_{298}(N_3)$ = 467 ± 8 kJ mol^{-1}.[4−7] The spin-allowed dissociation to $N(^2D)$ + $N_2(X\ ^1\Sigma_g^+)$ products is endoergic by 225 kJ mol^{-1};[6] however, dissociation to $N(^4S)$ + $N_2(X\ ^1\Sigma_g^+)$ products has $D_0(N - N_2)$ = −0.5 ± 1.0 kJ mol^{-1},[4,6] and the azide radical is stable only because this spin-forbidden dissociation pathway has an appreciable potential energy barrier. As a result, most azide radical reactions liberate large amounts of energy. Furthermore, azide radical reactions are often constrained by propensity rules to produce electronically excited species.[10−14] The possibility for the generation of electronically excited products has attracted considerable attention, but only a few studies have established rate constants and product branching ratios. In addition, there is a need to understand the reactions of delocalized π-type radicals, such as $N_3(\tilde{X}\ ^2\Pi_g$-$(1\sigma_g^2 2\sigma_g^2 1\sigma_u^2 3\sigma_g^2 2\sigma_u^2 4\sigma_g^2 3\sigma_u^2 1\pi_u^4 1\pi_g^3))$, as opposed to the better characterized reactions of σ-type radicals.

Azide radicals are typically produced in the gas phase via the reaction of fluorine atoms with hydrazoic acid, which follows one of two competing channels.

$$F + HN_3 \rightarrow N_3 + HF \qquad \Delta_r H^\circ_{298} = -180 \text{ kJ mol}^{-1} \quad (1)$$

$$F + HN_3 \rightarrow HNF + N_2 \qquad \Delta_r H^\circ_{298} = -263 \text{ kJ mol}^{-1} \quad (2)$$

The production of azide radicals has a rate constant k_1 = (1.1 ± 0.1) × 10^{-10} cm^3 $molecule^{-1}$ s^{-1}. Hewett and Setser[27] have shown that reaction 2 has a rate constant k_2 = (6.3 ± 3.5) × 10^{-12} cm^3 $molecule^{-1}$ s^{-1}, and hence reaction 1 is the dominant channel, with a branching fraction for the formation of N_3 of 0.97. The relative concentrations of azide radicals may be monitored via laser-induced fluorescence (LIF),[8,9] and that technique was employed here as a convenient monitor in a flow reactor to measure reaction rate constants.

The reactions of azide radicals have been previously studied with a variety of atomic partners, including F, Cl, Br, S, N, C, O, P, and As.[7,8,10−15,20,28−35] All of these reactants give some electronically excited products; however, only the reactions with halogen atoms[7,8] and nitrogen atoms[28,29] have high branching fractions for producing electronically excited products. A large body of work has used the reaction of N_3 with F atoms as the chemical source for $NF(a^1\Delta)$.[7,8,13−15] Currently, the focus has shifted to the reaction of N_3 with Cl atoms, since this reaction produces a high yield of electronically excited singlet $NCl(a^1\Delta)$ molecules with perhaps some $NCl(X^3\Sigma^-)$.[8,10−12,14,36]

$$\begin{aligned} N_3 + Cl &\rightarrow N_2 + NCl(a\ ^1\Delta) \quad \Delta_r H^\circ_{298} = -159 \text{ kJ mol}^{-1} \\ &\rightarrow N_2 + NCl(X\ ^3\Sigma^-) \qquad = -270 \text{ kJ mol}^{-1} \end{aligned} \quad (3)$$

A wide discrepancy exists in the values of k_3 reported by different laboratories. Liu et al.[8] reported a value of k_3 = (2.8 ± 0.4) × 10^{-10} cm^3 $molecule^{-1}$ s^{-1}, determined by monitoring the decrease in NF(a) intensity (formed via F + N_3) as Cl_2 was added to the reactor. A portion of the F atoms reacted with the Cl_2 to form Cl + ClF. Jourdain et al.[19,20] reported that k_3 lies between 0.75 and 1.5 × 10^{-11} cm^3 $molecule^{-1}$ s^{-1} on the basis of a comparison of a numerical simulation and experimental data for the reaction of Cl with ClN_3 using mass spectrometry

S1089-5639(98)01739-3 CCC: $15.00
Published on Web 07/09/1998

to monitor both N_3 and NCl. Two recent studies, by Henshaw and co-workers[37] and by Manke and Setser,[36] have studied the experimental kinetics of NF(a) and NCl(a) in the F/Cl/HN_3 system and support the smaller value of k_3. Resolving this discrepancy for k_3 is critical to understanding the generation of NCl(a) from the reaction of N_3 with Cl atoms, and a direct determination of k_3 was the main motivation of this investigation.

In this paper, the reaction kinetics of azide radicals have been investigated in a room-temperature flow reactor using laser-induced fluorescence (LIF) to monitor the relative concentration of the $N_3(\tilde{X}\ ^2\Pi_{3/2})$ state. The energy separation[17] between the two spin−orbit states of $N_3(\tilde{X})$ is only 71.9 cm^{-1}. We assumed equilibration between the two spin−orbit states in 0.5 Torr of Ar carrier gas, and the LIF signal was taken to be proportional to the total $[N_3]$. The excited state of azide, $N_3(\tilde{A}\ ^2\Sigma_u^+)$, lies above all three possible dissociation channels: 440 kJ mol^{-1} above the $N(^4S) + N_2$, 215 kJ mol^{-1} above the $N(^2D) + N_2$, and 100 kJ mol^{-1} above the $N(^2P) + N_2$ channel.[6] All vibrational levels of $N_3(\tilde{A})$ predissociate,[6,9] and $N(^2D) + N_2$ is the main product channel. Nevertheless, monitoring $[N_3]$ by LIF is still relatively straightforward for concentrations $\geq 1 \times 10^{11}$ molecules cm^{-3}. The reactions of N_3 with Cl atoms, F atoms, nitric oxide, molecular chlorine, oxygen, carbon monoxide, carbon dioxide, nitrogen dioxide, and propylene were examined. The rate of the reaction between azide and F atoms

$$N_3 + F \rightarrow N_2 + NF\ (a\ ^1\Delta) \qquad \Delta_r H^\circ_{298} = -183\ \text{kJ mol}^{-1} \tag{4}$$

has been established[7,8] to be $k_4 = (5 \pm 2) \times 10^{-11}$ cm^3 $molecule^{-1}$ s^{-1}, and this reaction was used as a calibration to confirm the reliability of our kinetic method.

We also investigated reaction 5, since N atoms are frequently present from N_2 impurity in the Ar carrier gas in discharge systems.

$$N_3(\tilde{X}\ ^2\Pi_g) + N(^4S) \rightarrow N_2(X\ ^1\Sigma_g^+) + N_2(B\ ^3\Pi_g) \quad \text{or} \quad N_2(W\ ^3\Delta_u) \qquad \Delta_r H^\circ_{298} = -235 \quad \text{or} \quad -234\ \text{kJ mol}^{-1} \tag{5}$$

The $N_2(B)$ and $N_2(W)$ states, which are strongly coupled by collisions,[38] are the only electronically excited states that are both energetically allowed and correlate to the reactant states. By monitoring the nitrogen first-positive $N_2(B\ ^3\Pi_g \rightarrow A\ ^3\Sigma_u^+)$ emission, we could determine the presence of nitrogen atoms. The $N_2(B)$ emission also is observed if the azide radical decomposes on the reactor walls.[15] The bimolecular self-destruction reaction 6 has not been characterized, and we tried to put some limits on this rate constant.

$$2N_3(\tilde{X}\ ^2\Pi_g) \rightarrow 2N_2(X\ ^1\Sigma_g^+) + N_2(A\ ^3\Sigma_u^+) \quad \text{or} \quad N_2(B\ ^3\Pi_g) \qquad \Delta_r H^\circ_{298} = -349 \quad \text{or} \quad -235\ \text{kJ mol}^{-1} \tag{6}$$

The accumulation of metastable $N_2(A)$ molecules via reactions 5 and 6 must be considered in complex kinetic environments, since their participation in energy transfer reactions with a variety of atoms and molecules is well-known.[39]

B. Experimental Methods

The reactions of F atoms with hydrazoic acid and the subsequent reactions of azide radicals were carried out in a flow reactor at room temperature. The relative $N_3(\tilde{X}\ ^2\Pi_{3/2})$ concentration was detected at a fixed point in the reactor using LIF in 0.5 Torr of Ar carrier gas. The flow reactor and LIF system used are described below.

Flow Reactor. The flow reactor was a 82 cm long, 50 mm diameter Pyrex tube. The flow reactor consisted of two distinct regions; a pre-reactor where azide radicals were generated via reaction 1 and the main reactor where the reactions of azide radicals occurred. The pre-reactor varied in length from 25 to 37 cm depending on the position of the reagent inlet. The distance between the pre-reactor and the observation zone, the main reactor, was 8−20 cm. The surface of the flow reactor was coated with halocarbon wax (Halocarbon Products, series 600) to prevent the loss of F, Cl, and N_3 on the reactor walls. The inlet tubes for the Ar carrier gas, the F atom source (CF_4), the HN_3, and the reagent gases were located in an aluminum flange attached via an O-ring joint to the front end of the reactor. The Ar carrier gas was added to the pre-reactor through a perforated ring, the F atoms through an 10 mm o.d. quartz tube, and the HN_3 through another perforated ring located at the exit of the F atom inlet. The reagent gases were added to the reactor via a 6 mm o.d. movable tube whose length extended 25−37 cm from the F/HN_3 inlets and marked the starting point of the reactor. The normal Ar pressure in the reactor was ∼0.54 Torr. The laser beam entered the reactor through a 22 cm long baffled sidearm and exited through a 40 cm long baffled sidearm. The sidearms had Brewster angle quartz windows and were located ∼45 cm downstream from the start of the pre-reactor. The fluorescence was collected through a quartz window located perpendicular to the sidearms. The reactor was pumped using a mechanical pump/blower combination, and a linear flow velocity of 6400 cm s^{-1} was achieved over the pressure range of 0.4−2 Torr. Except for the reaction of F + N_3, all of the reactions were carried out under conditions such that $[HN_3]_0 > [F]_0$ in order to ensure that the F atoms did not remove azide radicals.

The flow velocity in the reactor corresponds to a minimum reaction time of ∼4 ms in the pre-reactor. Under typical reaction conditions, this was sufficient to allow reaction 1 to proceed to ∼75% of completion before the addition of the reactant gas. The reactions of the azide radicals with added reagent occurred during the ∼3 ms time between the start of the reactor and the LIF detection zone. Longer reaction times in the pre-reactor and reactor could be obtained by throttling the pump.

The argon carrier gas was purified by passage through two cooled (196 K) molecular sieve filled traps. The F atoms were produced by passing an Ar/CF_4 mixture through a microwave discharge in an alumina tube. For CF_4 concentrations in the $(0.2-2.0) \times 10^{12}$ molecules cm^{-3} range, nearly complete dissociation (2F + CF_2) is achieved;[40,41] thus, $[F]_0 = 2[CF_4]$ was assumed. An Ar/Cl_2 mixture was passed through a second microwave discharge in a quartz tube to produce the Cl atoms. The dissociation efficiency of Cl_2 was determined by measuring the 308 nm emission intensity from the XeCl*(B) formed by reaction 7. The intensity is first-order in $[Cl_2]$ for concentrations $\leq 8 \times 10^{12}$ molecules cm^{-3}.

$$Xe(6s[3/2]_2) + Cl_2 \rightarrow XeCl^*(B, C) + Cl \tag{7}$$

The $Xe(6s[3/2]_2)$ was generated in situ by passing a Xe/Ar mixture through a hollow cathode dc discharge,[42−44] that was placed in the reactor just in front of the quartz LIF observation window. The $Xe(6s[3/2]_2)$ reacts with the Cl_2 in the flow reactor. When the microwave discharge on the Cl_2 inlet is turned on, the concentration of molecular chlorine is reduced and the XeCl* emission is also reduced. It has been shown in

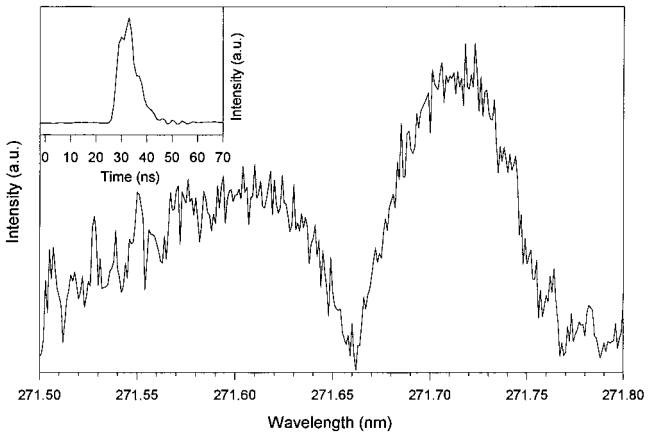

Figure 1. Laser-induced excitation spectrum of the $\tilde{A}\ ^2\Sigma_u^+(0,0,0) \leftarrow \tilde{X}\ ^2\Pi_{3/2}(0,0,0)$ transition of N_3. The fluorescence to the upper spin−orbit state $\tilde{X}\ ^2\Pi_{1/2}(0,0,0)$ was monitored at 272.5 nm. The reagent concentrations were $[Ar] = 1.7 \times 10^{16}$, $[CF_4] = 0.5 \times 10^{12}$, and $[HN_3] = 1.4 \times 10^{12}$ molecules cm^{-3}. The laser power was ~1 mJ/pulse, and 16 laser shots were averaged for each data point. The inset in the upper left corner shows a waveform following excitation of N_3 at 271.71 nm. The waveform, which is the average of 2048 separate laser shots, is the same as the decay time of the laser pulse, ~10 ns.

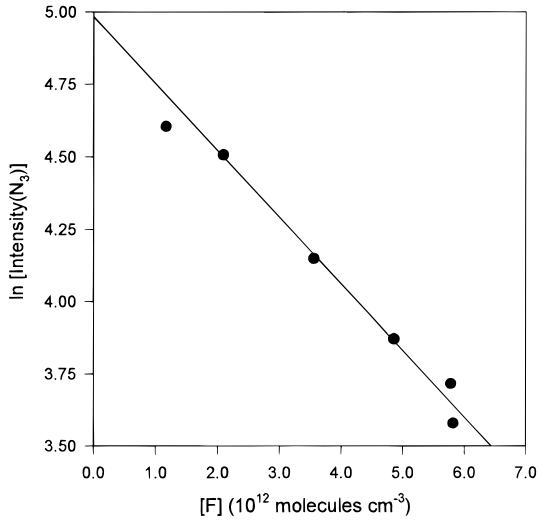

Figure 2. Logarithm of the relative azide LIF intensity vs fluorine atom concentration. The reactant concentrations used were $[Ar] = 1.7 \times 10^{16}$, $[HN_3] = 1.4 \times 10^{12}$, and $[CF_4] = (0.7-4.0) \times 10^{12}$ molecules cm^{-3}. The dissociation of CF_4 was assumed to give $[F]_0 = 2[CF_4]$. Using a reaction time of 2.6 ms, derived by assuming plug-flow behavior, the rate constant for reaction 4 is $(4.1 \pm 0.3) \times 10^{-11}$ cm^3 $molecule^{-1}$ s^{-1}. This compares favorably with the accepted value of $(5 \pm 2) \times 10^{-11}$ cm^3 $molecule^{-1}$ s^{-1}.

a similar reactor that the dissociation of Cl_2 is constant, yielding 0.6 Cl atoms per Cl_2 molecule.[45] The dissociation efficiency in our reactor was found to be consistent with the previously determined value of 0.6 Cl atoms per Cl_2 molecule.

The reagent gases were taken from commercial vendors and purified via freeze−pump−thaw cycles and stored as mixtures in argon. The HN_3 was prepared by the reaction of excess stearic acid with sodium azide (NaN_3) heated to 363 K under vacuum. The product, which was collected in a 12 L Pyrex reservoir, was diluted to 10% with argon. The flow rates of CF_4, HN_3, Cl_2, and the various reagent gases were controlled by stainless steel needle valves and measured by the pressure rise in a calibrated volume. The argon flow rate was controlled by needle valves and measured by a floating-ball flow meter that had been calibrated using a wet-test meter.

LIF System. The laser pulse was generated using a Nd:YAG laser (Quantel YG661S) pumped dye laser (Lambda Physik FL 3002) operating at 10 Hz. The frequency-doubled output of the dye laser gave <10 ns pulses with energies of ~1 mJ/pulse at 270 nm with a spectral bandwidth of 0.2 cm^{-1} using Coumarin 540 as the dye. The laser beam entered and exited the reactor via Brewster angle quartz windows on the sidearms. The fluorescence was detected using a 0.3 m monochromator (McPherson 218). A Hammamatsu R955 photomultiplier was attached to the exit slit of the monochromator, and the signal from the PMT was sent to a digital storage oscilloscope (Hewlett-Packard 54522A) operating under computer control. The same monochromator and PMT were used to acquire continuum spectra by switching to a photon-counting detection system.

The laser was used to excite the N_3 transition $\tilde{A}\ ^2\Sigma_u^+$ (0,0,0) ← $\tilde{X}\ ^2\Pi_{g,3/2}$ (0,0,0) from 271.5 to 271.8 nm, and the fluorescence to the upper spin−orbit state $\tilde{X}\ ^2\Pi_{g,1/2}$ (0,0,0) was monitored at 272.5 nm. The waveforms collected by the digital storage oscilloscope were integrated over the time interval of 25−80 ns. A typical excitation spectrum of N_3 together with a waveform is shown in Figure 1. The waveform is limited by the pulse width of the laser. The short lifetime of $N_3(\tilde{A})$, <10 ns, is a consequence of the predissociation.[6] The fluorescence intensity from a given $[N_3]$ was determined by integrating its LIF spectrum to determine the total area. About 10 min was required to scan a typical spectrum.

C. Experimental Results

The azide radicals were produced via reaction 1 using a dilute mixture of CF_4 in Ar passing through a microwave discharge as the source of F atoms. The system was operated with excess $[HN_3]$, except for the measurement of the F atom rate constant. Typical reactor pressures were 0.54 Torr, and the population distribution for N_3 was expected to be 300 K Boltzmann after ~4 ms of flow in the pre-reactor section. The primary source of uncertainty in the following results is due to the uncertainty in $[F]_0$ and Δt. After the Ar, F, and HN_3 enter the flow tube, they pass through the F + HN_3 pre-reaction zone, after which plug flow is established.

With careful alignment of the laser, azide spectra without contamination by scattered light were obtained. No background emission was observed that could be attributed to the $N_2(B)$. This indicates that decomposition of azide on the reactor walls was minimal and that N atom concentrations were unimportant. The $[N_3]$ used in these experiments ranged from 1 to 30.0×10^{12} molecules cm^{-3}. Scaling to higher azide concentrations is difficult owing to the high consumption of HN_3 and the desire to minimize the storage of HN_3, which is explosive.

N_3 + F. To determine the rate of reaction 4, Ar, HN_3, and CF_4 concentrations of 1.7×10^{16}, 1.4×10^{12}, and $(0.7-4.0) \times 10^{12}$ molecules cm^{-3}, respectively, were allowed to react. The CF_4 flow was divided into two portions; 0.7×10^{12} molecules cm^{-3} was added to the pre-reactor, and the remainder was added to the reactor. The dissociation of CF_4 was assumed to give $[F]_0 = 2[CF_4]$. Since $[F]_0 = [HN_3]$, all of the HN_3 was consumed in the pre-reactor. One determination of k_4 is shown in Figure 2. The average of two determinations of the rate constant k_4 was found to be $(4.1 \pm 0.3) \times 10^{-11}$ cm^3 $molecule^{-1}$ s^{-1}. This value compares favorably with the accepted value[7,8] of $(5 \pm 2) \times 10^{-11}$. The difference between the measured and accepted values are within the uncertainty of k_4. The value for k_4 is based upon the reaction time (2.6 ms) as calculated

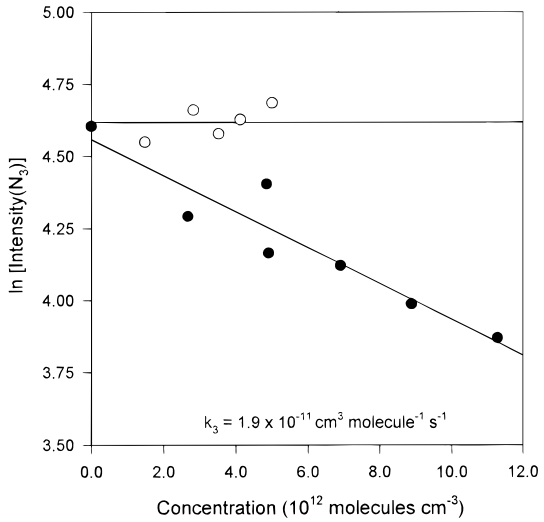

Figure 3. Logarithm of the relative azide fluorescence intensity vs molecular chlorine and atomic chlorine concentrations. In both cases, the reaction time was 2.6 ms. For molecular chlorine (○) the reactant concentrations used were [Ar] = 1.7×10^{16}, [CF_4] = 6.1×10^{11}, [HN_3] = 2.8×10^{12}, and [Cl_2] = $(1.0-5.0) \times 10^{12}$. The fluorescence intensity of N_3 remained constant within 10% as Cl_2 was added to the reactor. For atomic chlorine (●) the reactant concentrations used were [Ar] = 1.7×10^{16}, [HN_3] = 3.5×10^{12}, [CF_4] = 7.3×10^{12}, and [Cl_2] = $(2.5-18.8) \times 10^{12}$ molecules cm^{-3}; $[Cl]_0 = 0.6[Cl_2]$. The rate constant from this experiment for $N_3 + Cl$ is 1.9×10^{-11} cm^3 $molecule^{-1}$ s^{-1}.

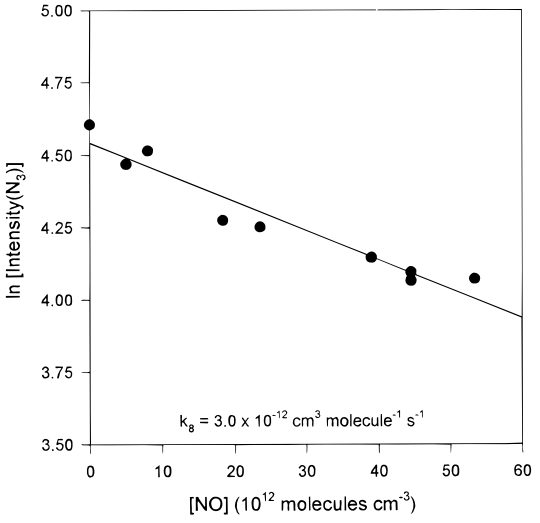

Figure 4. Logarithm of the relative azide LIF intensity vs nitric oxide concentration. The reactant concentrations were [Ar] = 1.8×10^{16}, [HN_3] = 3.0×10^{12}, [CF_4] = 8.7×10^{11}, and [NO] = $(0.0-53.4) \times 10^{12}$ molecules cm^{-3}. The rate constant for reaction 8 is $(2.9 \pm 0.3) \times 10^{-12}$ cm^3 $molecule^{-1}$ s^{-1} for $\Delta t = 3.4$ ms.

assuming plug flow in the main flow reactor (17 cm) and the uncertainty is the standard deviation obtained from the least-squares fit to the experimental data. The true reaction time could be slightly shorter than the calculated time because of incomplete mixing, but we will use the plug-flow value since the F-atom rate constant is acceptable.

Twelve potential energy surfaces correlate to the $F(^2P) + N_3(\tilde{X}\ ^2\Pi_g)$ asymptotic limit, disregarding the $J = {}^3/_2$ and ${}^1/_2$ spin−orbit states of F. Of these surfaces, only two correlate to the ground-state $FN_3(\tilde{X}\ ^1A')$. Assuming that reaction 4 passes through an $FN_3(\tilde{X})$ intermediate, that all the potentials are sampled statistically,[46] and that the activation energy is negligible, then the observed rate constant should be approximately the product of the gas kinetic constant, $\sim 3 \times 10^{-10}$ cm^3 $molecule^{-1}$ s^{-1}, and the fraction of the total number of potential energy surfaces that correlate to the intermediate $FN_3(\tilde{X}\ ^1A')$. This indicates that the rate constant should be approximately[46] ${}^2/_{12}$ $(3 \times 10^{-10}) = 5 \times 10^{-11}$ cm^3 $molecule^{-1}$ s^{-1}, in close agreement with the accepted value of k_4.

$N_3 + Cl_2$. The possibility of molecular chlorine reacting with azide was examined by adding Cl_2 to the reactor 9 cm before the LIF observation zone. Reactant concentrations of 1.7×10^{16}, 6.1×10^{11}, 2.8×10^{12}, and $(1.0-5.0) \times 10^{12}$ molecules cm^{-3} for Ar, CF_4, HN_3, and Cl_2, respectively, were used. The fluorescence intensity of N_3 remained constant as shown in Figure 3 for $\Delta t = 2.6$ ms indicating that no reaction was occurring. Under differing conditions, isolated points with [Cl_2] up to 1.7×10^{13} molecules cm^{-3} were examined. Again, no decrease in the fluorescence intensity of N_3 was observed upon the addition of Cl_2. This sets an upper limit for the rate constant of $\leq 0.5 \times 10^{-12}$ cm^3 $molecule^{-1}$ s^{-1}. This is reasonable since the reaction between azide and molecular chlorine to form chloroazide is actually 39 kJ mol^{-1} endoergic.[47]

$N_3 + Cl$. To determine k_3, a dilute flow of molecular chlorine was passed through a second microwave discharge, and the resulting Cl atoms were added 37 cm downstream from the entry of the F/Ar/HN_3 flows to the reactor just as for the F atom experiment. The dissociation efficiency of Cl_2 is constant for our concentration range and $[Cl]_0 = 0.6[Cl_2]$, e.g., 30% dissociation. Using reactant concentrations of 1.7×10^{16}, 7.3×10^{11}, 3.5×10^{12}, and $(2.5-18.8) \times 10^{12}$ molecules cm^{-3} for Ar, CF_4, HN_3, and Cl_2, respectively, the rate constant, k_3, as shown for the data in Figure 3, was found to be 1.9×10^{-11} cm^3 $molecule^{-1}$ s^{-1}. Five experimental determinations of k_3 were made, and the average value was $(2.1 \pm 0.6) \times 10^{-11}$ cm^3 $molecule^{-1}$ s^{-1}, where the uncertainty is the standard deviation of the five measurements. The absolute uncertainty in k_3 depends on the uncertainty in Δt and in $[Cl]_0$. The uncertainty in Δt includes a possible systematic error resulting from the finite mixing time of the reagents. Using the difference between the observed rate constant, k_4, for $F + N_3$ and the accepted value,[7,8] we estimate that Δt may be ~20% lower than the calculated plug-flow value. The estimated uncertainty in the dissociation efficiency of Cl_2 results in $[Cl]_0$ having an uncertainty of ±15%. The rate constant with uncertainty of reaction 3 is thus $(2.1^{+1.0}_{-0.6}) \times 10^{-11}$ cm^3 $molecule^{-1}$ s^{-1}.

This value compares favorably with the values reported by Jourdain et al.,[19,20] Henshaw et al.,[37] and Manke and Setser,[36] but it is an order of magnitude smaller than the value reported by Liu et al.[8] Further support for the lower value of k_3 may be obtained by comparing the observed rate constant for reaction 3 with the value estimated from the gas kinetic collision rate constant times the electronic branching fraction. As for $F + N_3$, 12 potential energy surfaces arise from the $Cl(^2P) + N_3(\tilde{X}\ ^2\Pi_g)$ asymptotic limit, and only two of these surfaces correlate to the ground-state $ClN_3(\tilde{X}\ ^1A')$. Assuming that reaction 3 passes through an $ClN_3(\tilde{X})$ intermediate, that all the potentials are sampled statistically, and that the activation energy is negligible, then an estimate of the rate constant may be obtained from the product of the gas kinetic constant, $\sim 3 \times 10^{-10}$ cm^3 $molecule^{-1}$ s^{-1}, and the fraction of the total number of potential energy surfaces that correlate to the intermediate $ClN_3(\tilde{X})$. This estimated value for k_3, 5×10^{-11} cm^3 $molecule^{-1}$ s^{-1}, is in rough agreement with our observed value, $(2.1^{+1.0}_{-0.62}) \times 10^{-11}$ cm^3 $molecule^{-1}$ s^{-1}. A more precise estimate of the electronic branching fraction should include the thermal distribution between $Cl(^2P_{3/2})$ and $Cl(^2P_{1/2})$ states and weighting of the triplet-state potentials.

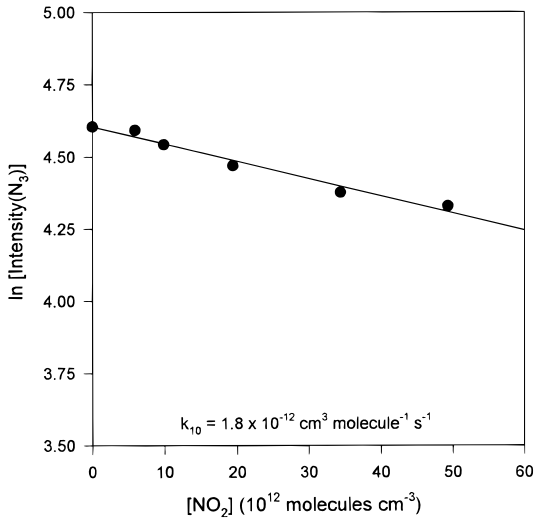

Figure 5. Logarithm of the relative azide LIF intensity vs nitrogen dioxide concentration. The reactant concentrations were [Ar] = 1.7×10^{16}, [HN_3] = 2.3×10^{12}, [CF_4] = 6.9×10^{11} and [NO_2] = (0.0−49.3) $\times 10^{12}$ molecules cm^{-3}. The rate constant for reaction 10 is (1.9 ± 0.2) $\times 10^{-12}$ cm^3 $molecule^{-1}$ s^{-1} for Δt = 3.4 ms.

N_3 + NO. Upon addition of nitric oxide to the reactor, a decrease in the LIF intensity of N_3 was observed. The reactant concentrations used to measure the rate constant were 1.8×10^{16}, 8.7×10^{11}, 3.0×10^{12}, and $\leq 5.4 \times 10^{13}$ molecules cm^{-3} for Ar, CF_4, HN_3, and NO, respectively. As shown in Figure 4, the rate constant was found to be 3.0×10^{-12} cm^3 $molecule^{-1}$ s^{-1}. Two determinations of k_8 were made, and the average rate constant was found to be (2.9 ± 0.3) $\times 10^{-12}$ cm^3 $molecule^{-1}$ s^{-1}.

The nitric oxide is probably abstracting a nitrogen atom from the azide radical to form N_2O.

$$N_3\,(\tilde{X}\,^2\Pi_g) + NO\,(X\,^2\Pi) \rightarrow N_2O + N_2 \qquad \Delta_r H^\circ_{298} = -480\ \text{kJ mol}^{-1} \quad (8)$$

A similar reaction is known to occur between NCO and NO.[48,49] In the case of NCO, the analogous reaction has two allowed pathways via an [ON−NCO] intermediate:

$$\begin{aligned} NCO\,(\tilde{X}\,^2\Pi) + NO\,(X\,^2\Pi) &\rightarrow N_2O + CO \qquad \Delta_r H^\circ_{298} = -278\ \text{kJ mol}^{-1} \\ &\rightarrow CO_2 + N_2 \qquad \Delta_r H^\circ_{298} = -643\ \text{kJ mol}^{-1} \end{aligned} \quad (9)$$

The intermediate either directly dissociates into N_2O + CO, or it isomerizes into a cyclic structure and then dissociates via a four-center transition state[49] into CO_2 + N_2. The direct dissociation pathway has a branching fraction of 0.44 and a rate constant of 1.45×10^{-11} cm^3 $molecule^{-1}$ s^{-1}, while the four-center dissociation pathway has a rate constant of 1.85×10^{-11} cm^3 $molecule^{-1}$ s^{-1}. When N_3 is substituted for NCO, both the direct dissociation and the four-center dissociation pathways will yield the same products, N_2O + N_2. In reactions 8 and 9, two π-type radicals are interacting to give linear closed-shell products. The N_3 reaction and one of the NCO reaction pathways can be imagined to proceed by transfer of a N(^{2}D) atom, thus conserving spin.

N_3 + NO_2. A decrease in the LIF intensity of N_3 was observed as the NO_2 concentration was increased in the flow reactor. The reactant concentrations used for the rate constant measurement were 1.7×10^{16}, 6.7×10^{11}, 2.3×10^{12}, and $\leq 4.9 \times 10^{13}$ molecules cm^{-3} for Ar, CF_4, HN_3, and NO_2, respectively. A complication to the determination of [NO_2] is the possible presence of N_2O_4 in the storage reservoir. By maintaining a partial pressure of NO_2 less than 0.5 Torr in both the pressure rise bulb and the flow reactor, we ensured that the N_2O_4 concentration was negligible. The data from one experiment, shown in Figure 5, resulted in a rate constant of 1.8×10^{-12} cm^3 $molecule^{-1}$ s^{-1}. From two separate experiments, the average rate constant k_{10} was found to be (1.9 ± 0.2) $\times 10^{-12}$ cm^3 $molecule^{-1}$ s^{-1}.

This interesting reaction can occur via several possible, highly exoergic reaction channels; the azide radical may undergo addition at either the nitrogen atom or at one of the oxygen atoms in NO_2.

$$\begin{aligned} N_3 + NO_2 &\rightarrow [N_2{-}N{-}ONO] \rightarrow 2NO + N_2 \qquad \Delta_r H^\circ_{298} = -325\ \text{kJ mol}^{-1} \\ &\rightarrow [N_2{-}N{-}NO_2] \rightarrow 2N_2O \qquad \Delta_r H^\circ_{298} = -341\ \text{kJ mol}^{-1} \\ &\rightarrow N_2 + N_2O + O \qquad \Delta_r H^\circ_{298} = -174\ \text{kJ mol}^{-1} \\ &\rightarrow 2N_2 + O_2 \qquad \Delta_r H^\circ_{298} = -505\ \text{kJ mol}^{-1} \end{aligned} \quad (10)$$

Comparison with the observed reaction channels in the analogous NCO + NO_2 reaction[50] allows us to elucidate the more probable reaction pathways. The thermodynamically allowed reactions for NCO + NO_2 are

$$\begin{aligned} NCO + NO_2 &\rightarrow [OCN{-}ONO] \rightarrow 2NO + CO \qquad \Delta_r H^\circ_{298} = -122\ \text{kJ mol}^{-1} \\ &\rightarrow [OCN{-}NO_2] \rightarrow N_2O + CO_2 \qquad \Delta_r H^\circ_{298} = -504\ \text{kJ mol}^{-1} \\ &\rightarrow NO + N + CO_2 \qquad \Delta_r H^\circ_{298} = -23\ \text{kJ mol}^{-1} \\ &\rightarrow N_2 + O_2 + CO \qquad \Delta_r H^\circ_{298} = -303\ \text{kJ mol}^{-1} \end{aligned} \quad (11)$$

Park and Hershberger[50] have examined reaction kinetics and product channels of the NCO + NO_2 reaction. They find that the major channel, N_2O + CO_2, accounts for ~92% of the observed products and occurs with a rate of 1.6×10^{-11} cm^3 $molecule^{-1}$ s^{-1}. This channel proceeds by isomerization of the $OCNNO_2$ intermediate into a four-centered cyclic form and then undergoes concerted dissociation. The minor channel proceeds via the OCNONO intermediate forming 2NO + CO with a rate constant of 1.4×10^{-12} cm^3 $molecule^{-1}$ s^{-1}. The other possible channels, involving further dissociation of the products or extensive rearrangement of the adduct, were not observed. An examination of the analogous reaction channels in the case of N_3 + NO_2 indicates that the most probable paths are the $2N_2O$ and the 2NO + N_2 channels. The channel forming nitrogen and oxygen would require rearrangement of the adduct formed by adding N_3 to the nitrogen and is, thus, considered to be a less probable reaction pathway.

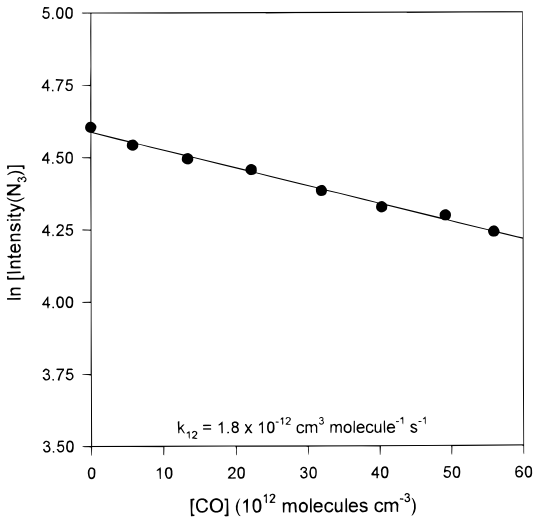

Figure 6. Logarithm of the relative azide intensity vs carbon monoxide concentration. The reactant concentrations were [Ar] = 1.7×10^{16}, [HN_3] = 3.1×10^{12}, [CF_4] = 6.7×10^{11}, and [CO] = $(0.0-55.9) \times 10^{12}$ molecules cm^{-3}. The rate constant for reaction 12 is $(1.8 \pm 0.1) \times 10^{-12}$ cm^3 $molecule^{-1}$ s^{-1} for $\Delta t = 3.4$ ms.

N_3 + CO. A decrease in the N_3 LIF intensity was observed as the CO concentration added to the flow reactor was increased. The reactant concentrations used for the rate constant study were 1.7×10^{16}, 6.7×10^{11}, 3.1×10^{12}, and $\leq 5.6 \times 10^{13}$ molecules cm^{-3} for Ar, CF_4, HN_3, and CO, respectively. The rate constant k_{12} was determined to be $(1.8 \pm 0.2) \times 10^{-12}$ cm^3 $molecule^{-1}$ s^{-1} from two experiments, one of which is shown in Figure 6.

This reaction results in the probable formation of NCO.

$$N_3 + CO \rightarrow NCO + N_2 \qquad \Delta_r H^\circ_{298} = -202 \text{ kJ mol}^{-1} \quad (12)$$

This reaction can be viewed as the transfer of a N(^{2}D) atom from N_3 to CO. Though this reaction probably produces NCO, it is less attractive than the F + HNCO[48] reaction as a flow reactor source of NCO, since two sequential reactions must occur to produce NCO. Nevertheless, reaction 12 still could be convenient in some applications, because HN_3 is easier to prepare and store than HNCO, and excess CO generally would not cause any kinetic problems in a flow reactor.

N_3 + CO_2, O_2, and Propylene. The addition of CO_2, O_2, or propylene to the flow reactor did not alter the LIF intensity of N_3. The reaction times in these experiments were 3.4 ms between the addition of the quenching agent and the laser interaction region. Figure 7 shows that the normalized LIF intensity of N_3 remained constant as the concentration of the quenching reagent was increased up to 1.0×10^{14} molecules cm^{-3}. This sets an upper bound on the rate constants of $\leq 5 \times 10^{-13}$ cm^3 $molecule^{-1}$ s^{-1}. Thus, azide radicals do not readily add to double bonds or react with oxygen. The result for O_2 is similar to that found in NCO reactions,[51] which has an upper bound of $\leq 5 \times 10^{-15}$ cm^3 $molecule^{-1}$ s^{-1}. However, the result for propylene differs from that found for NCO. Wategaonkar and Setser[48] obtained a rate constant of 2.4×10^{-11} cm^3 $molecule^{-1}$ s^{-1} for NCO + C_3H_6, which is at least 48 times faster than the rate for N_3 + C_3H_6 found in this work. One explanation for the greater reactivity of NCO toward unsaturated molecules, as opposed to N_3, is the difference in electron localization. NCO has the π-antibonding electrons more localized on the nitrogen end of the radical,[52] making it more reactive toward addition at the N end to the double bond, while in the case of N_3, the electron density will be distributed symmetrically over the radical.

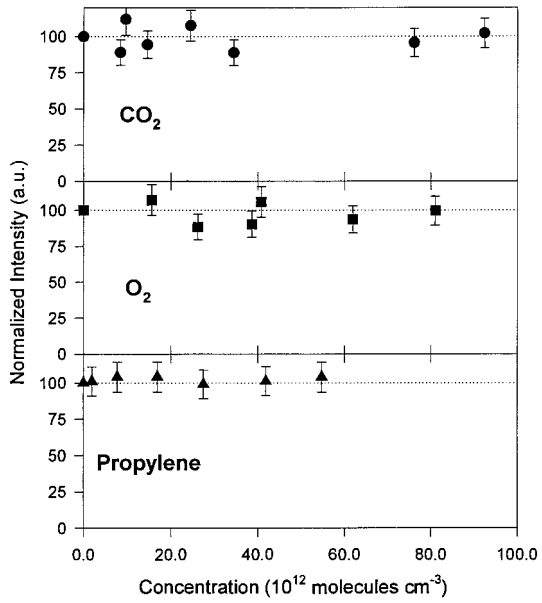

Figure 7. Normalized fluorescence intensity of N_3 as function of added quenching reagent. The reactant concentration were (●) [Ar] = 1.7×10^{16}, [HN_3] = 2.5×10^{12}, [CF_4] = 6.9×10^{11}, [CO_2] = $(0.0-92.4) \times 10^{12}$; (■) [Ar] = 1.7×10^{16}, [HN_3] = 2.6×10^{12}, [CF_4] = 5.8×10^{11}, [O_2] = $(0.0-81.0) \times 10^{12}$; or (▲) [Ar] = 1.7×10^{16}, [HN_3] = 4.7×10^{12}, [CF_4] = 9.4×10^{11}, [propylene] = $(0.0-54.8) \times 10^{12}$ molecules cm^{-3}. In all three cases, no observed quenching occurs.

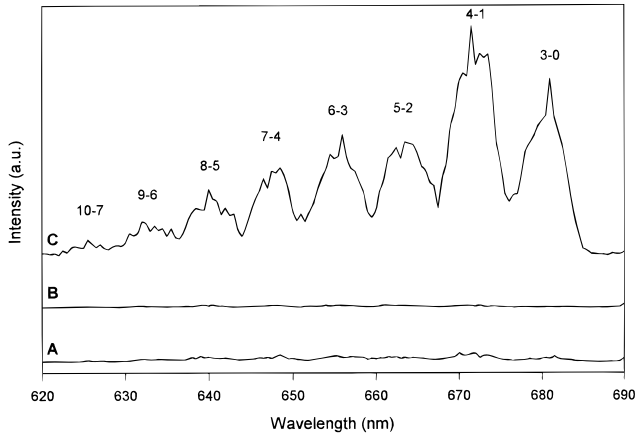

Figure 8. N_2(B−A) emission spectrum for the $\Delta v = -3$ sequence from N atoms, formed by passing N_2 through a microwave discharge, reacting with N_3. The reagent concentrations were [Ar] = 6.8×10^{16}, [CF_4] = 6.7×10^{12}, [HN_3] = 1.3×10^{13}, and [N_2] = 1.1×10^{14} molecules cm^{-3}. Spectra were collected under three different conditions: (A) without any nitrogen atoms added to the system, (B) without any azide in the system, and (C) with both nitrogen atoms and azide.

N_3 + N and 2N_3. Nitrogen atoms were created by passing N_2 through a microwave discharge. Upon addition of the N atoms to the reactor with N_3, strong emission from the N_2(B $^3\Pi_g \rightarrow$ A $^3\Sigma_u^+$) bands was observed. As shown in Figure 8, this emission was absent if either the azide radicals or the nitrogen atoms were removed from the flow reactor. Furthermore, the LIF intensity of the azide radical was reduced upon addition of N atoms. In fact, previous researchers[28,29] have determined the rate of reaction 5 to be 1.6×10^{-11} cm^3 $molecule^{-1}$ s^{-1}. Since other laboratories have studied N + N_3, we did not measure [N] to obtain the rate constant k_5. These results are a strong indication that reaction 5 is of no significance in our reactor without added N atoms. The principle source of N atoms in flow reactors occurs from either air contamination

of the Ar carrier gas or from wall-induced decomposition of azide radicals.[40] Careful gas-handling techniques eliminate the possibility of air contamination. The absence of emission from $N_2(B)$ without the addition of N atoms shows that wall-induced decomposition of azide radicals is negligible in our wax-coated reactor.

The bimolecular removal of azide via reaction 6 was examined by increasing both [F] and [HN_3] to achieve [N_3] $\leq 1.3 \times 10^{13}$ molecules cm^{-3}. The LIF signal was observed to scale linearly with azide concentration, and the first-positive emission was not observed. Since the LIF remained proportional to the azide concentration and no $N_2(B, \Delta v = 3)$ emission was observed, we conclude that the rate for this reaction is below our detection limit. For a second-order reaction, and assuming we could see 10% reduction in [N_3] for a reaction time of 6 ms, the rate constant is $\leq 2 \times 10^{-12}$ cm^3 molecule^{-1} s^{-1}. A comparison was made between the observed emission intensities from reactions 5 and 6 in order to obtain a second estimate of the k_6 rate constant. Using a steady-state analysis, the ratio of the first-positive emission from reactions 5 and 6 is proportional to

$$\frac{I_5}{I_6} = \frac{k_5[\mathrm{N}][\mathrm{N_3}]}{\tau_\mathrm{B}^{-1}} \cdot \frac{\tau_\mathrm{B}^{-1}}{k_6[\mathrm{N_3}]^2} = \frac{k_5[\mathrm{N}]}{k_6[\mathrm{N_3}]} \qquad (13)$$

where I is the emission intensity and τ_B is the lifetime of $N_2(B)$. Assuming that the dissociation of N_2 is ~5% and that the emission from reaction 5 as shown in Figure 8 is only 10 times the detection limit, then reaction 13 gives $k_6 \leq 7 \times 10^{-13}$ cm^3 molecule^{-1} s^{-1} for [N_3] $= 1.3 \times 10^{13}$ and [N] $= 5.5 \times 10^{12}$ molecules cm^{-3}. A separate series of measurements was then performed using a different flow reactor in order to lengthen the reaction time and use higher [N_3]. This reactor, designed for the study of NCl(a) kinetics,[36] consisted of a 70 mm Pyrex tube 120 cm in length. The detector consisted of a 0.5 m monochromator with a cooled (193 K) S-1 photomultiplier tube that could be moved along the length of the reactor. We used the $\Delta v = 0$ transition from 900 to 100 nm for observation. Using [N_3] $\leq 3 \times 10^{13}$ molecules cm^{-3} and a reaction time of $\leq$100 ms, we searched for emission from $N_2(B)$. Even with the highest [N_3], no $N_2(B)$ emission was observed. Our conclusion reduces the rate constant reported by Jourdain and co-workers[19,20] who estimated a value for k_6 based upon the reduction of [N_3], as measured by mass spectrometry, to be $(5-8) \times 10^{-11}$ cm^3 molecule^{-1} s^{-1}. Yamasaki et al.[28a] also correlated the ratio of $N_2(B)$ emission from reactions 5 and 6 to arrive at a rate of 1.4×10^{-12} cm^3 molecule^{-1} s^{-1}. This was obtained from eq 13 by measuring a ratio of 95:1 for the $N_2(B)$ emission with and without added N atoms.[28b] Their measurement is consistent with our result, and the bimolecular self-destruction constant of N_3 at 298 K is small and probably less than 1×10^{-12} cm^3 molecule^{-1} s^{-1}.

The bimolecular removal of NCO was observed by Wategaonkar and Setser[48]

$$2\mathrm{NCO} \rightarrow [\mathrm{OCN{-}NCO}] \rightarrow \mathrm{N_2} + 2\mathrm{CO}$$
$$\Delta_r H^\circ_{298} = -540 \text{ kJ mol}^{-1} \qquad (14)$$

and a rate constant of $(5.0 \pm 2.0) \times 10^{-12}$ cm^3 molecule^{-1} s^{-1} was assigned. The rates of reactions 6 and 14 are both slow, relative to most radical−radical reactions, which usually have rate constants close to the collision limit times an electronic branching factor. Of course, N_3 and NCO cannot simply recombine to form a stable molecule, and evidently the delocalization of the electron density leads to a small activation energy for the recombination−decomposition process.

The vibrational distribution of the $N_2(B)$ emission from reaction 5 was compared with similar emission formed from the reaction

$$2\mathrm{N}(^4\mathrm{S}) + \mathrm{Ar} \rightarrow \mathrm{N_2}(\mathrm{X}\ ^1\Sigma_g^+, \mathrm{A}\ ^3\Sigma_u^+, \mathrm{B}^3\Pi_g, \mathrm{W}\ ^3\Delta_u) + \mathrm{Ar}$$
$$\Delta_r H^\circ_{298} = -945, -350, -236, \quad \text{or} \quad -235 \text{ kJ mol}^{-1} \qquad (15)$$

The [N_2] passed through the discharge was ~10 times greater for reaction 15 than that used for reaction 5. The $\Delta v = -3$ sequence from the $N_2(B\ ^3\Pi_g \rightarrow A\ ^3\Sigma_u^+)$ emission observed from reactions 5 and 15 was compared, and the observed vibrational distributions were the same regardless of whether the source of the excited nitrogen molecules was reaction 5 or 15 in 2 Torr of Ar. We believe that this result arises from the fact that both reactions have the same thermochemistry and that vibrational relaxation and collisionally induced mixing[38,39] between the A, B, and W states give the same steady-state $N_2(B)$ distribution at pressures of ~2 Torr. This precludes the use of the nitrogen first-positive emission as a diagnostic test to distinguish between reactions 5 and 15. The absence of any detectible $N_2(B\ ^3\Pi_g \rightarrow A\ ^3\Sigma_u^+)$ emission from reaction 6 also precludes its use as a diagnostic for [N_3] for concentrations of interest in a flow reactor.

D. Conclusions

Some controversy has arisen over the rate of reaction between Cl and N_3. This study, which directly monitored the reduction in azide concentration as a function of added Cl utilizing LIF of N_3, found a rate constant of $(2.1^{+1.0}_{-0.6}) \times 10^{-11}$ cm^3 molecule^{-1} s^{-1} at 298 K. This confirms the rate constant value determined by Jourdain and co-workers[19,20] and the value favored by observing NCl(a) and NF(a) in direct competition.[36,37] Coombe reported a rate constant for reaction 3 that is more than an order of magnitude larger. This overestimate must be a consequence of the experimental method, which measured the decrease in [NF(a)] with added [Cl] that was obtained from the reaction of F atoms with Cl_2. The NF(a) concentration decayed in the flow reactor, and extrapolations were made to zero time to estimate the NF(a) from the competition between N and Cl atoms for N_3. Perhaps the NF(a) decay rate was more complicated than expected based on the extrapolation. The rate constant for reaction 3 should be less than or equal to the collision limit multiplied by the electronic branching fraction of the entrance channel. Assuming that the reaction passes through an $ClN_3(\tilde{X})$ intermediate, then k_3 should be $<\sim 5 \times 10^{-11}$ cm^3 molecule^{-1} s^{-1}.

The NO, NO_2, and CO reactions were observed to occur with measurable rates. The reaction between N_3 and NO has a rate constant of $(2.9 \pm 0.3) \times 10^{-12}$ cm^3 molecule^{-1} s^{-1} and probably produces N_2O and N_2 by N atom transfer. The reaction between N_3 and CO has a rate constant of $(1.8 \pm 0.2) \times 10^{-12}$ cm^3 molecule^{-1} s^{-1}, producing NCO as the primary product. NO_2 probably reacts with N_3 to form either two N_2O molecules or two NO molecules and N_2. This reaction has a rate constant of $(1.9 \pm 0.2) \times 10^{-12}$ cm^3 molecule^{-1} s^{-1}. No reaction was observed between Cl_2, CO_2, O_2 and propylene molecules and azide radicals, which sets a limit for $k \leq 5 \times 10^{-13}$ cm^3 molecule^{-1} s^{-1}.

The reactions of N_3 and NCO are similar, as one would expect for these two isoelectronic species. However, the N_3 reactions studied in this work are slower than the corresponding reactions

of NCO; the reactions with NO, NO_2, and propylene are, at least, 1 order of magnitude slower. This is an indication that N_3 is less reactive than NCO. The bimolecular self-removal reaction rates of the π-type radicals, N_3 and NCO, are rather slow; the rate constants are $\leq 1-2 \times 10^{-12}$ and 5×10^{-12} cm^3 $molecule^{-1}$ s^{-1} respectively. These rate constants are much smaller than the corresponding reactions of σ-type radicals, such as CH_3. In addition to the delocalization of the odd-electron density, the reactions of N_3 and NCO do not give a stable adduct molecule, and these recombination reactions are rather slow. Thus, rather high concentrations of N_3 and NCO can be created and used.

Acknowledgment. This work was supported by the U.S. Air Force under Grant F49620-96-1-0110 from the Air Force Office of Scientific Research.

References and Notes

(1) Petrongolo, C. *J. Mol. Struct.* **1988**, *175*, 215−220.
(2) Kaldor, U. *Int. J. Quantum Chem., Quantum Chem. Symp.* **1990**, *24*, 291−294.
(3) Chambaud, G.; Rosmus, P. *J. Chem. Phys.* **1992**, *96*, 77−89.
(4) Martin, J. M. L.; François, J. P.; Gijbels, R. *J. Chem. Phys.* **1990**, *93*, 4485−4487.
(5) Pellerite, M. J.; Jackson, R. L.; Brauman, J. I. *J. Phys. Chem.* **1981**, *85*, 1624−1626.
(6) Continetti, R. E.; Cyr, D. R.; Osborn, D. L.; Leahy, D. J.; Neumark, D. M. *J. Phys. Chem.* **1993**, *99*, 2616−2631.
(7) Habdas, J.; Wategaonkar, S.; Setser, D. W. *J. Phys. Chem.* **1987**, *91*, 451−458.
(8) Liu, X.; MacDonald, M. A.; Coombe, R. D. *J. Phys. Chem.* **1992**, *96*, 4907−4912.
(9) Beaman, R. A.; Nelson, T.; Richards, D. S.; Setser, D. W. *J. Phys. Chem.* **1987**, *91*, 6090−6092.
(10) Clark, T. C.; Clyne, M. A. A. *Trans. Faraday Soc.* **1970**, *66*, 877−885.
(11) Pritt, A. T., Jr.; Coombe, R. D. *Int. J. Chem. Kinet.* **1980**, *12*, 741−753.
(12) Clyne, M. A. A.; MacRobert, A. J.; Brunning, J.; Cheah, C. T. *J. Chem. Soc., Faraday Trans. 2* **1983**, *79*, 1515−1524.
(13) Coombe, R. D.; Pritt, A. T., Jr. *Chem. Phys. Lett.* **1978**, *58*, 606−610.
(14) Pritt, A. T., Jr.; Patel, D.; Coombe, R. D. *Int. J. Chem. Kinet.* **1984**, *16*, 977−993.
(15) David, S. J.; Coombe, R. D. *J. Phys. Chem.* **1986**, *90*, 3260−3263.
(16) Thrush, B. A. *Proc. R. Soc. London Ser. A* **1956**, *235*, 143−147.
(17) Douglas, A. E.; Jones, W. J. *Can. J. Phys.* **1965**, *43*, 2216−2221.
(18) Clark, T. C.; Clyne, M. A. A. *Trans. Faraday Soc.* **1969**, *65*, 2994−3004.
(19) Combourieu, J.; Le Bras, G.; Poulet, G.; Jourdain, J. L. *Reaction Cl + N_3Cl and Reactivity of N_3, NCl and NCl_2 Radicals in Relation to the Explosive Decomposition of N_3Cl*; Sixteenth Symposium (International) on Combustion, 1976, Massachusetts Institute of Technology, Cambridge, MA.
(20) Jourdain, J. L.; Le Bras, G.; Poulet, G.; Combourieu, J. *Combust. Flame* **1979**, *34*, 13−17.
(21) Dyke, J. M.; Jonathan, N. B. H.; Lewis, A. E.; Morris, A. *Mol. Phys.* **1982**, *47*, 1231−1240.
(22) Pahnke, R.; Ashworth, S. H.; Brown, J. M. *Chem. Phys. Lett.* **1988**, *147*, 179−182.
(23) Tian, R.; Facelli, J. C.; Michl, J. *J. Phys. Chem.* **1988**, *92*, 4073−4079.
(24) Continetti, R. E.; Cyr, D. R.; Metz, R. B.; Neumark, D. M. *Chem. Phys. Lett.* **1991**, *182*, 406−411.
(25) Haas, T.; Gericke, K.-H.; Maul, C.; Comes, F. J. *Chem. Phys. Lett.* **1993**, *202*, 108−114.
(26) Henshaw, T. L.; Herrera, S. D.; Haggquist, G. W.; Schlie, L. A. V. *J. Phys. Chem. A* **1997**, *101*, 4048−4056.
(27) Hewett, K. B.; Setser, D. W. *J. Phys. Chem. A* **1997**, *101*, 9125−9131.
(28) (a) Yamasaki, K.; Fueno, T.; Kajimoto, O. *Chem. Phys. Lett.* **1983**, *94*, 425−429. (b) The enthalpy of formation of N_3 used by the authors is now considered obsolete. Using the currently accepted value, the allowed vibrational excitation of the N_2(B) products arising from reactions 5 and 6 would be identical. In addition, the emission intensity from reaction 6 observed by the authors is extremely weak.
(29) David, S. J.; Coombe, R. D. *J. Phys. Chem.* **1985**, *89*, 5206−5212.
(30) Henshaw, T. L.; MacDonald, M. A.; Stedman, D. H.; Coombe, R. D. *J. Phys. Chem.* **1987**, *91*, 2838−2842.
(31) Henshaw, T. L.; McElwee, D.; Stedman, D. H.; Coombe, R. D. *J. Phys. Chem.* **1988**, *92*, 4606−4610.
(32) Henshaw, T. L.; Ongstad, A. P.; Lawconnell, R. I. *J. Phys. Chem.* **1990**, *94*, 3602−3609.
(33) Quiñones, E.; Dagdigian, P. J. *J. Phys. Chem.* **1992**, *96*, 2201−2205.
(34) May, D. J.; Coombe, R. D. *J. Phys. Chem.* **1989**, *93*, 520−525.
(35) Piper, L. G.; Krech, R. H.; Taylor, R. L. *J. Chem. Phys.* **1979**, *71*, 2099−2104.
(36) Manke, G., II.; Setser, D. W. *J. Phys. Chem. A* **1998**, submitted.
(37) Henshaw, T. L.; Herrera, S. D.; Schlie, L. A. V. *J. Phys. Chem. A* **1998**, in press.
(38) Sadeghi, N.; Setser, D. W. *J. Chem. Phys.* **1983**, *79*, 2710−2726.
(39) Golde, M. F. *Int. J. Chem. Kinet.* **1988**, *20*, 75−92.
(40) Du, K. Y.; Setser, D. W. *J. Phys. Chem.* **1991**, *95*, 4728−4735.
(41) Du, K. Y.; Setser, D. W. *J. Phys. Chem.* **1992**, *96*, 2553−2561.
(42) Sobczynski, R.; Setser, D. W.; Slagle, A. R. *J. Chem. Phys.* **1990**, *92*, 1132−1144.
(43) Sobczynski, R.; Setser, D. W. *J. Chem. Phys.* **1991**, *95*, 3310−3324.
(44) Zhong, D.; Setser, D. W.; Sobczynski, R.; Gadomski, W. *J. Chem. Phys.* **1996**, *105*, 5020−5036.
(45) Manke, G. C., II.; Setser, D. W. *J. Phys. Chem. A* **1998**, *102*, 153−159.
(46) The 12 potential surfaces consist of 2 ^{1}A′, 4 ^{1}A″, 2 ^{3}A′, and 4 ^{3}A″. We did not weigh the triplet surfaces by their multiplicity. Doing so would reduce the fraction of states that correlate to the FN_3 intermediate to $^1/_{18}$ and thus produce a lower estimate for the F + N_3 rate constants.
(47) Paillard, C.; Moreau, R.; Combourieu, J. *C. R. Acad. Sci. C* **1967**, *264*, 832.
(48) Wategaonkar, S.; Setser, D. W. *J. Phys. Chem.* **1993**, *97*, 10028−10034.
(49) Cooper, W. F.; Park, J.; Hershberger, J. F. *J. Phys. Chem.* **1993**, *97*, 3283−3290.
(50) Park, J.; Hershberger, J. F. *J. Phys. Chem.* **1993**, *97*, 13647−13652.
(51) Atakan, B.; Wolfrum, J. *Chem. Phys. Lett.* **1991**, *178*, 157−162.
(52) The oxygen atom in NCO is more electronegative (and has a higher ionization energy) than the nitrogen atom. As a consequence the π_u bonding molecular orbital will have greater electron density on the oxygen atom. The π_g antibonding molecular orbital will have greater electron density on the nitrogen atom.